

# Zonal Organization of the Vestibulocerebellum in Pigeons (*Columba livia*): I. Climbing Fiber Input to the Flocculus

IAN R. WINSHIP<sup>1</sup> AND DOUGLAS R.W. WYLIE<sup>1,2\*</sup>

<sup>1</sup>Department of Psychology, University of Alberta, Edmonton, Alberta T6G 2E9, Canada

<sup>2</sup>Division of Neuroscience, University of Alberta, Edmonton, Alberta T6G 2E9, Canada

---

---

## ABSTRACT

Previous studies in pigeons have shown that the neurons in the medial column of the inferior olive respond best to patterns of optic flow resulting from self-rotation. With respect to the axis of rotation, there are two functional groups: *rVA* neurons prefer rotation about the vertical axis, whereas *rH45* neurons respond best to rotation about an horizontal axis oriented at 45 degrees ipsilateral azimuth. The *rVA* and *rH45* neurons are located in the caudal and rostral margins of the medial column, respectively. These olivary neurons project as climbing fibers to the contralateral flocculus. In this study, injections of anterograde tracers into the medial column were used to investigate the zonal organization of the climbing fiber input to the flocculus of pigeons. Iontophoretic injections of either cholera toxin subunit-B or biotinylated dextrin amine were made into the medial column of the inferior olive at locations responsive to *rVA* or *rH45* rotational optic flow. Anterogradely labeled climbing fibers in the flocculus showed a clear zonal organization. There were four parasagittal bands spanning both folia IXcd and X consisting of two *rVA* zones interdigitated with two *rH45* zones. These findings are compared with the zonal organization of the flocculus in mammalian species. *J. Comp. Neurol.* 456:127–139, 2003. © 2002 Wiley-Liss, Inc.

**Indexing terms:** vestibulocerebellum; inferior olive; optokinetic; optic flow; anterograde tracer

---

---

The complex spike activity (CSA) of Purkinje cells in the pigeon vestibulocerebellum responds best to patterns of optic flow that result from self-motion. In the medial half of the vestibulocerebellum, CSA responds best to optic flow patterns resulting from self-translation (Wylie et al., 1993, 1998; Wylie and Frost, 1999a). In the lateral half of the vestibulocerebellum, the flocculus, CSA responds best to optic flow resulting from self-rotation. The rotation cells in the flocculus respond best to rotational optic flow about one of two axes in three-dimensional space: either the vertical axis or an horizontal axis oriented at 45 degrees contralateral azimuth/135 degrees ipsilateral azimuth (Wylie and Frost, 1993). We refer to these two response types as *rVA* and *rH45* neurons, respectively (Wylie, 2001; Winship and Wylie, 2001). This finding was first shown in a series of studies in rabbits by Simpson, Graf, and colleagues by using optic flow patterns produced by a rotating planetarium projector (Simpson et al., 1981, 1988a; Graf et al., 1988). They emphasized that the rotational optokinetic system is organized with respect to a three-axis reference frame that is common to the vestibular

canals and the eye muscles (Simpson and Graf, 1981, 1985; Ezure and Graf, 1984; Graf et al., 1988; Leonard et al., 1988; Simpson et al., 1988a,b, 1989a,b; van der Steen et al., 1994; see also Wylie and Frost, 1996). In fact, the translation cells in the medial vestibulocerebellum are also organized with respect to this three-axis reference frame (Wylie et al., 1998; Wylie and Frost, 1999a).

In the rabbit flocculus, the *rVA* and *rH45* Purkinje cells are (1) organized into parasagittal zones that receive climbing fiber (CF) input from distinct regions of the inferior olive (IO), and (2) have differential projections to the

---

Grant sponsor: Natural Sciences and Engineering Research Council.

\*Correspondence to: Douglas R. W. Wylie, Department of Psychology, University of Alberta, Edmonton, Alberta T6G 2E9, Canada.  
E-mail: dwylie@ualberta.ca

Received 6 December 2001; Revised 23 July 2002; Accepted 25 September 2002

DOI 10.1002/cne.10507

Published online the week of December 16, 2002 in Wiley InterScience (www.interscience.wiley.com).

cerebellar and vestibular nuclei (Leonard et al., 1988; Ruigrok et al., 1992; De Zeeuw et al., 1994; Tan et al., 1995). The *rVA* neurons are found in two zones (zones FZ<sub>II</sub> and FZ<sub>IV</sub>) that are interdigitated with two zones that contain *rH45* neurons (zones FZ<sub>I</sub> and FZ<sub>III</sub>; De Zeeuw et al., 1994; Tan et al., 1995). There is a fifth zone, zone C2, where the CSA is unresponsive to optokinetic stimulation (De Zeeuw et al., 1994). The *rVA* zones receive CF input from the caudal dorsal cap (dc), whereas the *rH45* zones receive CF input from the rostral dc and ventrolateral outgrowth (vlo; Tan et al., 1995). A similar organization of floccular Purkinje cells into parasagittal zones has been confirmed in several other mammalian species (cat, Gerrits and Voogd, 1982; rat, Ruigrok et al., 1992; monkey, Hess and Voogd, 1986; Voogd et al., 1987a,b; for a review, see Voogd et al., 1996).

Previous research in pigeons using retrograde transport from the vestibulocerebellum has shown that the *rVA* and *rH45* Purkinje cells receive CF input from discrete regions of the contralateral medial column of the IO (mcIO; Wylie et al., 1999). Similar to the connections in mammals, *rVA* and *rH45* neurons in the pigeon flocculus receive input from the caudal and rostral margins of the mcIO, respectively (Wylie et al., 1999). However, the zonal organization of the *rVA* and *rH45* Purkinje cells in the pigeon flocculus has yet to be determined. In the present study, we examined the zonal organization of CF projections with iontophoretic injections of anterograde tracers in the rostral and caudal mcIO in pigeons.

## MATERIALS AND METHODS

The methods reported herein conformed to the guidelines established by the Canadian Council on Animal Care and were approved by the Biosciences Animal Care and Policy Committee at the University of Alberta. Silver King and Homing Pigeons (obtained from a local supplier) were anesthetized with a ketamine (65 mg/kg) - xylazine (8 mg/kg) cocktail (i.m.). Supplemental doses were administered as necessary. The animals were placed in a stereotaxic device with pigeon ear bars and beak adapter so that the orientation of the skull conformed to the atlas of Karten and Hodós (1967). Access to the mcIO was achieved by removing bone and dura on the right side of the head over the cerebellum. Glass micropipettes, filled

with 2 M NaCl and having tip diameters of 4–5  $\mu\text{m}$ , were advanced through the cerebellum and into the brainstem to record the activity of neurons in the mcIO. Electrodes were oriented 10 degrees to the sagittal plane and advanced by using a hydraulic microdrive (Frederick Haer & Co.) in an attempt to access areas of the mcIO sensitive to rotational optic flow. Neurons in the medial margin of the mcIO respond best to rotational optic flow, whereas neurons in the lateral half of the mcIO respond to translational optic flow (see also Lau et al., 1998; Wylie et al., 1999; Crowder et al., 2000; Winship and Wylie, 2001). The *rVA* and *rH45* neurons are located in the caudal and rostral mcIO, respectively (Wylie et al., 1999; Winship and Wylie, 2001). Extracellular signals were amplified, filtered, and fed to a window discriminator, which produced transistor-transistor logic (TTL) pulses, each representing a single spike time. TTL pulses were fed to a data analysis system (Cambridge Electronic Designs (CED) *1401plus*) and peristimulus time histograms (PSTHs) were constructed by using *Spike2* software (CED).

IO cells were easily identified based on a low firing rate of approximately 1 spike/sec. After a cell was isolated, the optic flow preference was determined by using various procedures. These included simply listening to the response to moving a large (90 degrees  $\times$  90 degrees) hand-held stimulus, consisting of dots, lines, and squiggles, in various areas of the visual field, or quantifying the responses to panoramic optic flow produced by a planetarium projector. This device, modeled after that of Simpson et al. (1981), and the procedure for its use has been described in detail elsewhere (Wylie and Frost, 1993, 1999b). The device consisted of a small cylinder pierced with numerous small holes. A light source was positioned inside the cylinder such that dots were projected onto the walls, floor, and ceiling of the room. The cylinder was rotated about its long axis by a pen motor that was controlled by a function generator, thus producing rotational optic flow. The planetarium was suspended just above the bird's head in gimbals such that the axis of rotation could be positioned to any orientation in three-dimensional space. The cylinder oscillated at 0.1 Hz and a constant speed of 1 degree/sec. Generally, we found that the most convenient way to confirm the flowfield preference was to use a computer-generated large-field stimulus and a procedure that is illustrated in Figure 1A (Winship and Wylie, 2001).

### Abbreviations

An	nucleus angularis	mcIO	medial column of the inferior olive
BDA	biotinylated dextran amine	ml	molecular layer
CbL	lateral cerebellar nucleus	nXII	nucleus of the hypoglossal nerve
CbM	medial cerebellar nucleus	OCT/oct	olivocerebellar tract
CE	external cuneate nucleus	PCV	cerebellovestibular process
CF	climbing fiber	PH	plexus of Horsley
Cnd	central nucleus of the medulla oblongata, pars dorsalis	Pl	Purkinje layer
Cnv	central nucleus of the medulla oblongata, pars ventralis	R	Raphe nucleus
CSA	complex spike activity	RL	lateral reticular nucleus
CTB	cholera toxin subunit B	Rpc	parvocellular reticular nucleus
dc	dorsal cap	Ta	tangential nucleus
dl	dorsal lamella	TS	tractus solitarius
FLM	medial longitudinal fasciculus	TTD	nucleus of the descending trigeminal tract
gl	granule layer	VDL	dorsolateral vestibular nucleus
IO	inferior olive	VeD	descending vestibular nucleus
La	nucleus laminaris	VeS	superior vestibular nucleus
LS	spinal lemniscus	vl	ventral lamella
mc	medial column	vlo	ventrolateral outgrowth

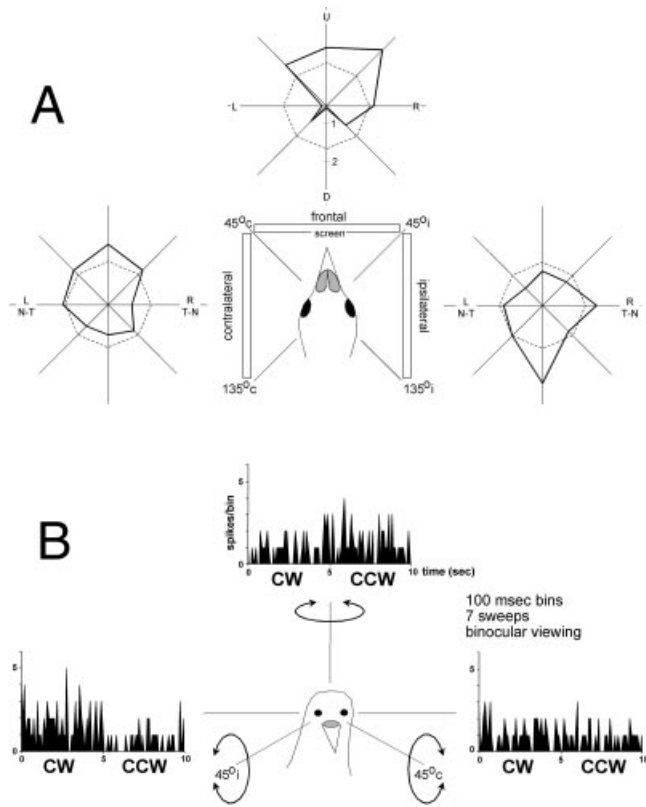


Fig. 1. Largefield and optic flow stimulation of neurons in mcIO. **A:** The direction tuning of the CSA for an *rH45* neuron is shown. Cell type was confirmed by obtaining direction tuning curves in response to drifting gratings backprojected onto a screen that was positioned in one of three locations relative to the bird's head: the frontal visual field (from 45 degrees ipsilateral (i) to 45 degrees contralateral (c) azimuth), the contralateral hemifield (from 45 degrees c to 135 degrees c azimuth), or the ipsilateral hemifield (from 45 degrees i to 135 degrees i azimuth). Firing rate (solid line, in spikes/sec relative to the spontaneous rate) is plotted as a function of the direction of motion in polar coordinates. Spontaneous firing rate is represented by the dotted circle. This neuron was excited in response to largefield stimuli moving upward in the contralateral and frontal visual fields and downward motion in the ipsilateral visual field (the neuron was in the right mcIO). **B:** The responses of an *rH45* neuron to the panoramic optic flow produced by the planetarium projector is shown. Peristimulus time histograms (PSTHs) are shown for the response to rotational optic flow about three axes: the vertical axis and two horizontal axes oriented 45 degrees to the midline. U, D, L, R represent upward, downward, leftward, and rightward movement of the gratings, respectively; T-N, temporal-to-nasal; N-T, nasal-to-temporal; CW, clockwise optic flow; CCW, counterclockwise optic flow. For other abbreviations, see list.

A screen measuring 90 degrees  $\times$  75 degrees (width  $\times$  height) was positioned in one of three locations relative to the bird's head: the frontal visual field (from 45 degrees ipsilateral (i) to 45 degrees contralateral (c) azimuth), the contralateral hemifield (from 45 degrees c to 135 degrees c azimuth), or the ipsilateral hemifield (from 45 degrees i to 135 degrees i azimuth). Drifting square wave or sine wave gratings of an effective spatial and temporal frequency were generated by a VSGThree (Cambridge Research Services) and back-projected (*InFocus* LP750) onto the screen. Direction tuning curves in each of the three areas of the visual field were obtained by moving the gratings in eight

different directions, 45 degrees apart. Responses were averaged over at least three sweeps, where each sweep consisted of 5 seconds of motion in one direction, a 5-second pause, and 5 seconds of motion in the opposite direction, followed by a 5-second pause. Although this procedure did not necessarily elicit maximal modulation of the cell, it was quite useful for identifying *rVA* and *rH45* cells. When recording from the IO on the right side of the brain, *rVA* neurons respond best to forward (temporal to nasal; T-N), rightward, and backward (N-T) motion in the contralateral, frontal, and ipsilateral visual fields, respectively, whereas *rH45* neurons respond best to upward motion in the contralateral and frontal fields, and downward motion in the ipsilateral field (Winship and Wylie, 2001).

After identification of a neuron in mcIO as either *rVA* or *rH45*, the recording electrode was replaced with a glass micropipette (tip diameter, 10–20  $\mu$ m) containing an anterograde tracer. In five cases, low-salt cholera toxin subunit B (CTB; Sigma, St. Louis, MO; 1% in 0.1 M phosphate-buffered saline [PBS, pH 7.4]) was iontophoretically injected for 1–3 minutes (+4  $\mu$ A, 7 seconds ON, 7 seconds OFF). In all other cases ( $n = 3$ ), biotinylated dextran amine (BDA; Molecular Probes; molecular weight = 10,000; 10% in 0.1 M phosphate buffer [PB; pH = 7.4]) was iontophoretically injected (+3  $\mu$ A, 1 second ON, 1 second OFF) for between 2 and 5 minutes. After the injection, the electrode was left undisturbed for an additional 5 minutes.

After a survival time of 3 to 5 days, the animals were given an overdose of sodium pentobarbital (100 mg/kg) and perfused with saline (0.9%) followed by ice-cold paraformaldehyde (4% in 0.1 M phosphate buffer [PB, pH 7.4]). The brains were extracted and post-fixed for 2–12 hours (4% paraformaldehyde, 20% sucrose in 0.1 M PB) and placed in sucrose overnight (20% in 0.1 M PB). The brain was then embedded in gelatin (10%) and placed back in the sucrose until the block sank. Frozen sections, 45  $\mu$ m thick, were collected in the coronal plane. The BDA or CTB was visualized by using a cobalt chloride intensification of diaminobenzidine. These procedures have been described in detail elsewhere (BDA, Wylie et al., 1997; CTB, Lau et al., 1998; see also Wild, 1993; Veenman et al., 1992). The tissue was mounted on gelatin chrome aluminum coated slides, lightly counterstained with Neutral Red, and examined by using light microscopy.

The photomicrographs shown in Figure 2 were taken by using a compound light microscope (Olympus Research Microscope BX60) equipped with a digital camera (Media Cybernetics CoolSNAP-Pro color digital camera). Adobe Photoshop software was used to compensate for brightness and contrast.

## Nomenclature

The avian cerebellum consists of a vermis without hemispheres, as is characteristic of mammalian species (Larsell, 1948; Larsell and Whitlock, 1952; Whitlock, 1952). The pigeon vestibulocerebellum consists of the two most ventral folia of the posterior vermis: IXcd and X using the nomenclature in Karten and Hodoss (1967), which we use, or IXb and X, according to Arends and Zeigler (1991). Generally, folia IXcd and X are referred to as the uvula and nodulus, respectively (Larsell, 1948; Larsell and Whitlock, 1952; Whitlock, 1952). These folia extend laterally and rostrally to form the auricle of the cerebellum, which has been referred to as the parafloccu-

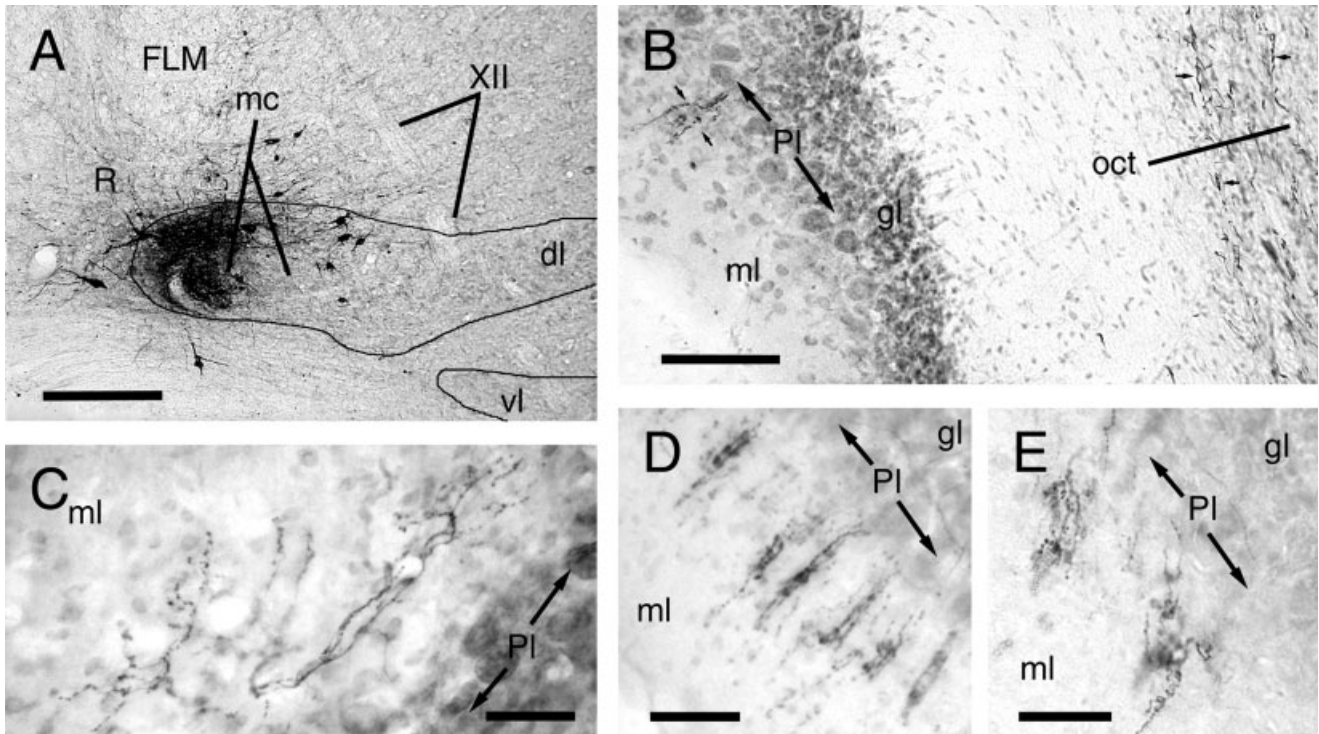


Fig. 2. Photomicrographs of an injection site and labeled CFs in the flocculus. **A:** A photomicrograph of a typical BDA injection site in the mcIO (case *rH45BDA2*). **B–E:** Anterogradely labeled CFs in the flocculus. In B, a CF in the molecular layer (ml) of the ventral auricle is highlighted. In addition, labeled fibers in the olivocerebellar tract

(oct) can be seen on the right-hand side, just medial to the dorsolateral vestibular nucleus (VDL). B and E were from BDA injections, whereas C and D were from CTB injections. XII, twelfth cranial nerve. For other abbreviations, see list. Scale bars = 250  $\mu\text{m}$  A, 100  $\mu\text{m}$  B, 50  $\mu\text{m}$  C–E.

lus and/or flocculus (Larsell, 1948; Larsell and Whitlock, 1952; Whitlock, 1952). We define the flocculus as the lateral part of folia IXcd and X where the CSA responds to rotational optic flow. More medially, CSA responds best to translational optic flow (Wylie et al., 1993, 1998; Wylie and Frost, 1999a). The division between the rotation and translation cells in the vestibulocerebellum is quite distinct. The border resides 1.65–1.9 mm from the midline in folium X, and 1.9–2.1 mm from the midline in folium IXcd (see Fig. 11 of Wylie et al., 1993). By using CTB as a retrograde tracer, it has been shown that the olivary cells projecting to the translation areas of the vestibulocerebellum reside immediately lateral to those that project to the flocculus (Lau et al. 1998; Crowder et al., 2000). What we refer to as the flocculus corresponds to zone F described by Arends and Zeigler (1991), except the lateral unfoliated cortex found rostral to the auricle. We define the auricle as the part of the flocculus that is rostral to the point where the invagination between folia IXcd and X disappears (see Figs. 3G, 8H).

## RESULTS

Experiments were performed in eight pigeons. Before injection in mcIO, optic flow preference was reliably recorded and quantitatively identified as either the *rVA* or the *rH45* response type. Generally, we found two or three cells of the same optic flow preference on a given penetration. We never found *rVA* and *rH45* cells on the same

track. The direction tuning of the CSA for an *rH45* neuron in response to gratings drifting in the frontal, ipsilateral, and contralateral regions of the visual field is shown in Figure 1A. Firing rate (spikes/sec relative to the spontaneous rate) is plotted as a function of the direction of motion in polar coordinates. This neuron was excited in response to largefield stimuli moving upward in the contralateral and frontal visual fields, and downward motion in the ipsilateral visual field (the neuron was in the right mcIO). Responses of an *rH45* neuron to the planetarium projector is illustrated in Figure 1B. This neuron (in the right IO) showed clear modulation to rotational optic flow about an axis oriented at 45 degrees ipsilateral azimuth. Much less modulation was seen to rotation about the vertical axis, and no modulation was seen to rotation about an horizontal axis oriented at 45 degrees contralateral azimuth.

Figure 2A shows a photomicrograph of a typical BDA injection site in the mcIO (case *rH45BDA2*). Compared with the BDA injection sites, the CTB injection sites were larger and the boundaries were not as well demarcated. Anterogradely labeled CF terminals were consistently found in the vestibulocerebellum contralateral to the injection sites. Figure 2B–E shows anterogradely labeled CFs in the flocculus. Consistent with Freedman et al. (1977), the terminals were restricted to the basal half of the molecular layer. In Figure 2B, a CF in the molecular layer of the ventral auricle is highlighted. In addition, labeled fibers in the olivocerebellar tract (OCT) can be

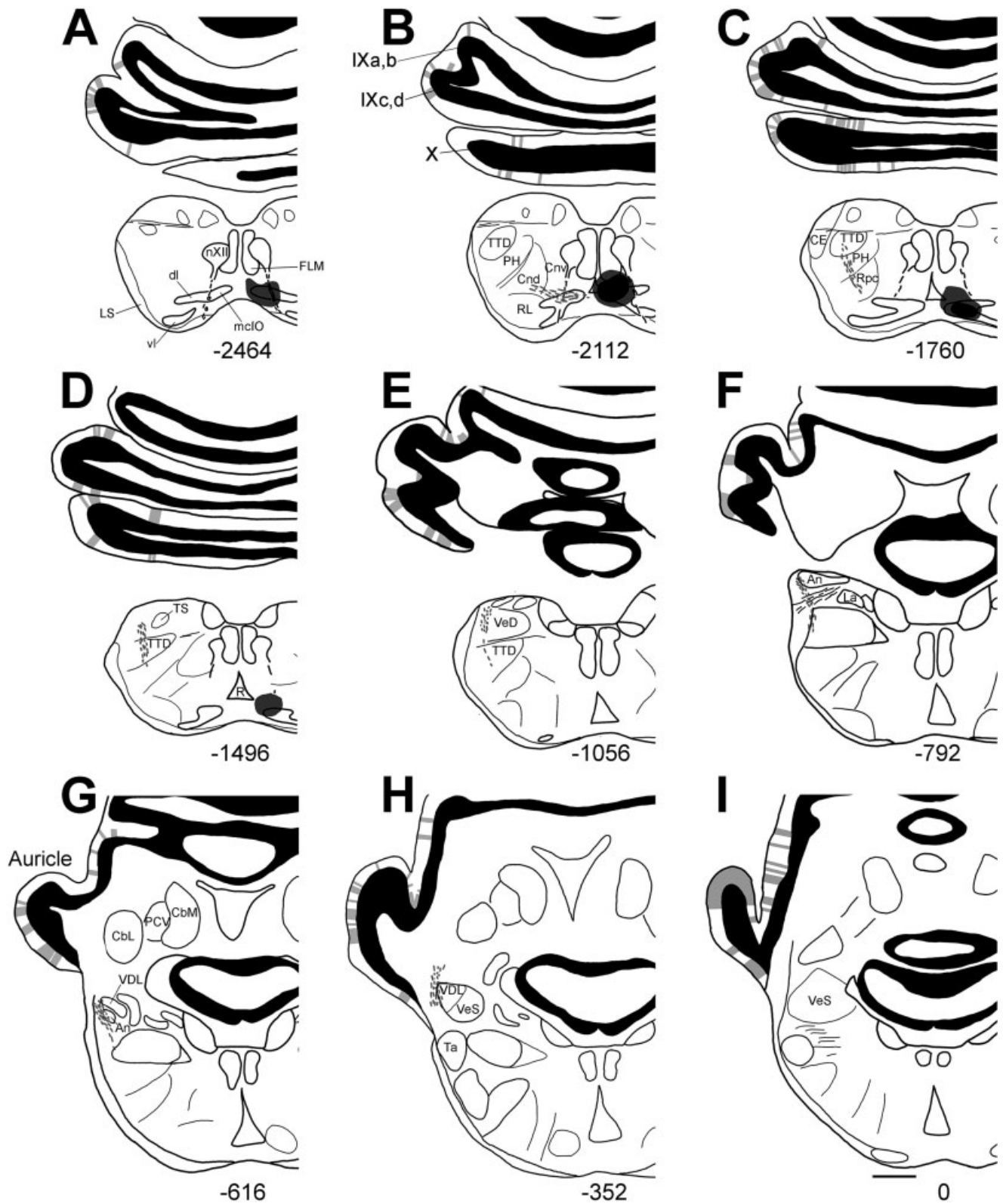
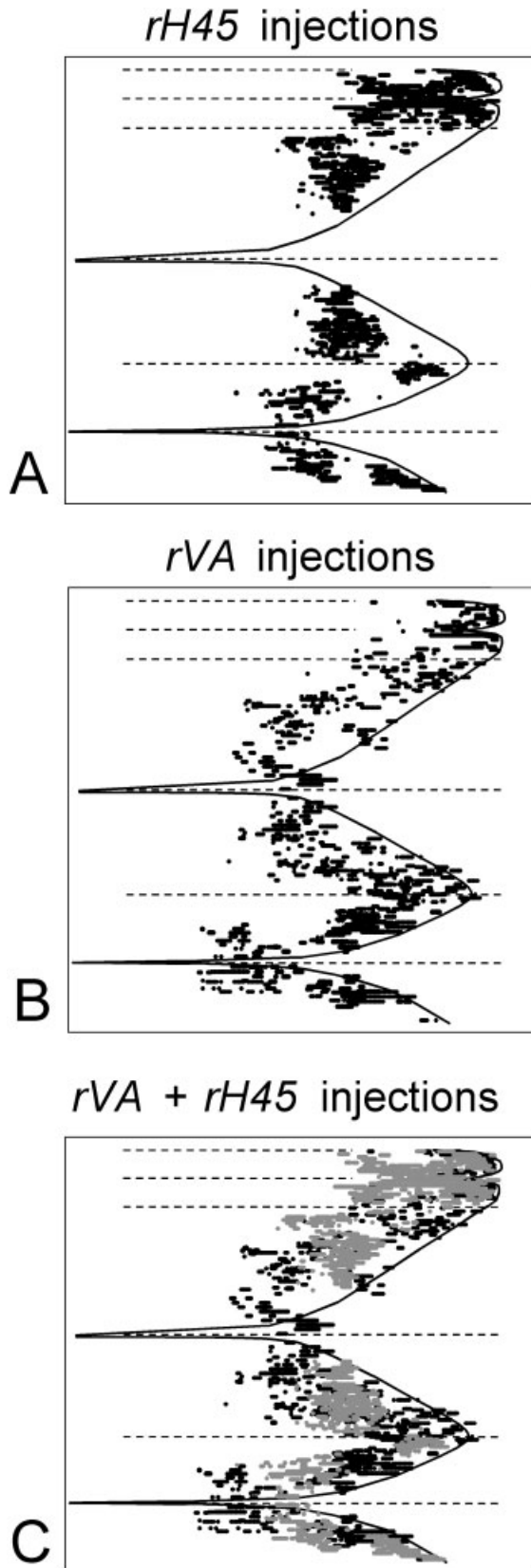


Fig. 3. Reconstruction of case *rH45CTB2*. Camera lucida drawings from caudal (A) to rostral (I) are shown. The distance ( $\mu\text{m}$ ) of each section from the rostral-most section is indicated at the bottom. The injection site is shown in more detail in Figure 5D. Labeled fibers crossed the midline at the injection site (Fig. 3B) and travelled later-

ally, dorsally, and rostrally as the olivocerebellar tract (OCT). The labeled climbing fiber terminals are shown as shading in the molecular layer in the cerebellar cortex. For other abbreviations, see list. Scale bar = 1 mm in I (applies to A-I).



seen on the right-hand side, just medial to the dorsolateral vestibular nucleus. Figure 2B,E was from BDA injections, whereas Figure 2C,D was from CTB injections.

Figure 5 shows drawings of the injection sites from all eight experiments. The BDA injection sites (Fig. 5B,E,H) were easy to illustrate as they were a uniform dark brown or black with well demarcated borders and surrounded by a much lighter penumbra. These are faithfully drawn in Figure 5. The CTB injection sites (Fig. 5C,D,F,G,I) were not as easy to illustrate. Although black at the center the borders were not as clear, and a gradation of gray radiated from the injection site. Moreover, the degree of labeling at the CTB injection sites varied from case to case. Nonetheless, we have attempted to use a similar scheme to draw the CTB injections: the black indicates the centers of the injections, and the surrounding gray indicates the apparent spread. We were very liberal with our estimates of the apparent spread. The injection sites of CTB injections were generally much larger than BDA injections and resulted in a greater amount of CF labeling in the flocculus. For the four cases illustrated on the top (Fig. 5B–E), *rH45* responses were recorded at the injection site, whereas *rVA* responses were recorded at the injection sites illustrated on the bottom (Fig. 5F–I). As expected from previous studies (Wylie et al., 1999; Winship and Wylie, 2001), there was a rostrocaudal separation of the *rH45* and *rVA* injection sites.

Figure 5A shows the functional topography of neurons sensitive to translational and rotational optic flow in the mcIO from previous neuroanatomic and electrophysiological studies (Wylie et al., 1999; Crowder et al., 2000; Winship and Wylie, 2001). The rostral (dark gray) and caudal (light gray) areas of the medial part of the mcIO contain *rH45* and *rVA* neurons, respectively (Wylie et al., 1999; Winship and Wylie, 2001). The lateral parts of the mcIO (cross-hatching) contain the neurons that respond to translational optic flow and project to the ventral uvula and nodulus (Lau et al., 1998; Wylie and Frost, 1999a; Crowder et al., 2000). There are actually four different types of translation neurons. They are topographically organized in the mcIO and project to different zones within folia IXcd and X (ventral uvula and nodulus; see Wylie and Frost, 1999a; Crowder et al., 2000). The most ventromedial portion of the mcIO, (i.e., that area not shaded in Fig. 5A), along with parts of the ventral lamella, project to zone E of the cerebellar cortex (Arends and Voogd, 1989; Lau et al., 1998). Zone E spans the lateral edge of all folia outside the vestibulocerebellum. The topographical organization of the mcIO illustrated in Figure 5A was useful for predicting which regions of the mcIO

Fig. 4. Collapsed and normalized data for all cases. Because of the variability in the size of the across birds, especially with respect to folium X, the rostrocaudal and mediolateral dimensions were first normalized before plotting. **A:** The four *rH45* cases are collapsed. Two clear zones in the flocculus emerge: one at rostralateral extent of folia IXcd and X and extending through the auricle, and a second caudomedial zone. **B:** The four *rVA* cases are collapsed. In folium X, two zones emerge: a rostralateral zone and a caudomedial zone. The data for folium IXcd are less clear. **C:** The data from the *rH45* cases (i.e., A) are superimposed on top of the data from the *rVA* cases (i.e., B). *rH45* and *rVA* data are represented by light gray and black circles, respectively. Although considerable overlap occurred, two *rH45* zones appear to be interdigitated with two *rVA* zones.

were involved in the injection because of spread of the tracer outside the target area.

### Case *rH45CTB2*

Figure 3 shows camera lucida drawings of nine coronal sections from case *rH45CTB2*. The injection site, the largest of the *rH45* injections, was found rostrally in the mcIO and is shown in more detail in Figure 5D. Although centered in the *rH45* region, there was apparent considerable spread, encroaching caudally into the *rVA* region and laterally to include some of the translation regions. In Figure 3, CF terminals are shown as shading in the molecular layer of the cerebellar cortex, and the route of the CFs to the cerebellum (the OCT described by Arends and Voogd, 1989), is shown. Fibers from the injection site crossed the midline at the injection site and coursed laterally through the contralateral mcIO (Fig. 3B). The fibers continued laterally through the ventral region of the central nucleus of the medulla oblongata, along the dorsal border of the lateral reticular nucleus (Fig. 3B). The fibers then turned dorsally and continued rostrally through the parvocellular reticular nucleus, the plexus of Horsley, and the nucleus of the descending trigeminal tract (Fig. 3C,D). Upon reaching the vestibular nuclear complex, the fibers continued dorsally and rostrally along the lateral edge of the descending vestibular nucleus, passed through the fibers innervating the tangential nucleus, then coursed along the lateral edge of nucleus angularis and the dorsolateral vestibular nucleus (Fig. 3E–H). Now in the cerebellum, the fibers fanned out: some traveled laterally to enter the auricle, whereas other turned caudally, most heading to the white matter of the vestibulocerebellum.

As expected from the location of the injection site, CF terminals in the molecular layer were found laterally in folia IXcd and X (i.e., the flocculus, Fig. 3A–F) and the auricle (Fig. 3G–I). Fewer terminals were found more medially in the ventral uvula and nodulus (e.g., ventral X in Fig. 3B,C), and some were also found laterally in folia VIII and IXab (Fig. 3E–I). This finding corresponds to zone E described by Arends and Voogd (1989), which receives input from the ventromedial mcIO (Arends and Voogd, 1989; Lau et al., 1998). There were also some very faintly labeled CF terminals in zone E of folia III, IV and V (not shown).

A zonal organization of the CF terminals in the vestibulocerebellum is apparent in Figure 3, but this is better illustrated in with the transformation in Figure 6B. This image shows the locations of anterogradely labeled CFs in the molecular layers of the vestibulocerebellum plotted on an “unfolded” sheet. Both the distance from the midline, measured under the microscope, and the rostrocaudal locations, based on the section number, are indicated. This representation is quite faithful, requiring a single transformation. The auricle, which is continuous with the rostralateral ends of folia IXcd and X (Fig. 3), has been split with a horizontal slice separating it into its dorsal and ventral aspects and is plotted as continuous with the dorsal IXcd. Plots of these measurements are shown for all *rH45* and *rVA* cases in Figures 6 and 7, respectively. The solid lines indicate the radii of the Purkinje layers, and the dark dots show the location of labeled CFs.

For case *rH45CTB2*, anterogradely labeled CFs in the flocculus are plotted in Figure 6B. Folium X was unusually large in this case (4.5 mm wide), but there were three clear zones (see also Fig. 3B–F). One zone was located at

the lateral extreme, centered 4.0 mm from the midline, a second zone was centered approximately 2.8 mm from the midline, and a third zone was centered approximately 1.7 mm from the midline. We believe that the most medial zone is due to spread of the injection upon the translation regions in the mcIO. (As mentioned above, the border between the translation cells and the rotation cells in folium X is approximately 1.65–1.9 mm from the midline [Wylie et al., 1993]). In folium IXcd there were two clear zones: a rostralateral zone that occupied the auricle (see also Fig. 3G–I), and a second caudomedial zone centered approximately 3.0 mm lateral to the midline (see also Fig. 3A–E). A few labeled CFs were found medially in ventral IXcd, possibly due to encroachment of the injection into the *rVA* region (see below).

### Case *rH45CTB1*

The injection site for this case, shown in Figure 5C, was relatively large. Although it was centered in the *rH45* region, there was considerable spread, encroaching caudally into the *rVA* region and laterally to include the translation regions. Anterogradely labeled CFs observed in the vestibulocerebellum are plotted in Figure 6A. The pattern of labeling was remarkably similar to case *rH45CTB2*. In folium X, there were three clear zones. One zone was on the lateral edge of the folium, centered approximately 3.75 mm lateral to the midline, and a second was centered approximately 2.5 mm from the midline. A third zone was centered approximately 1.3 mm from the midline. These resemble the three zones in folium X from case *rH45CTB2* but on a slightly smaller scale. The medial zone is consistent with encroachment of the injection on the translation regions of the mcIO. The labeling in folium IXcd was also similar to that observed in case *rH45CTB2*. Across both the dorsal and ventral lamellae, there was a rostralateral zone that occupied the auricle and a second caudomedial zone centered approximately 3.0 mm from the midline. There was also a little labeling more medially. In ventral IXcd, there was a small group centered 1.6 mm from the midline, medial to the translation/rotation border, and consistent with encroachment of the injection on the translation regions. In dorsal IXcd, there was a small group centered approximately 2.2 mm from the midline. Labeling in this region was typical of *rVA* injections (see below). Outside the vestibulocerebellum, there were some faintly labeled CF terminals in folium IXab, laterally, corresponding to the E zone, and more medially, corresponding to the C zone (Arends and Voogd, 1989).

### Case *rH45BDA1*

The injection site for this case, shown in Figure 5B, was relatively compact. It was centered in the heart of the *rH45* region and the spread was minimal. The location of anterogradely labeled CFs are plotted in Figure 6C. There were two distinct bands in folium X, one at the rostral extreme, centered approximately 3.5 mm from the midline, and a second more medially, centered approximately 2.3 mm from the midline. (Folium X was rather small in this case, ~3.7 mm wide.) There appeared to be two zones in folium IXcd: one rostralateral zone occupied the auricle, and a second caudomedial zone, centered approximately 3.1 mm from the midline. There was a single CF terminal observed outside the vestibulocerebellum. It was faintly labeled and found in folium IXab.

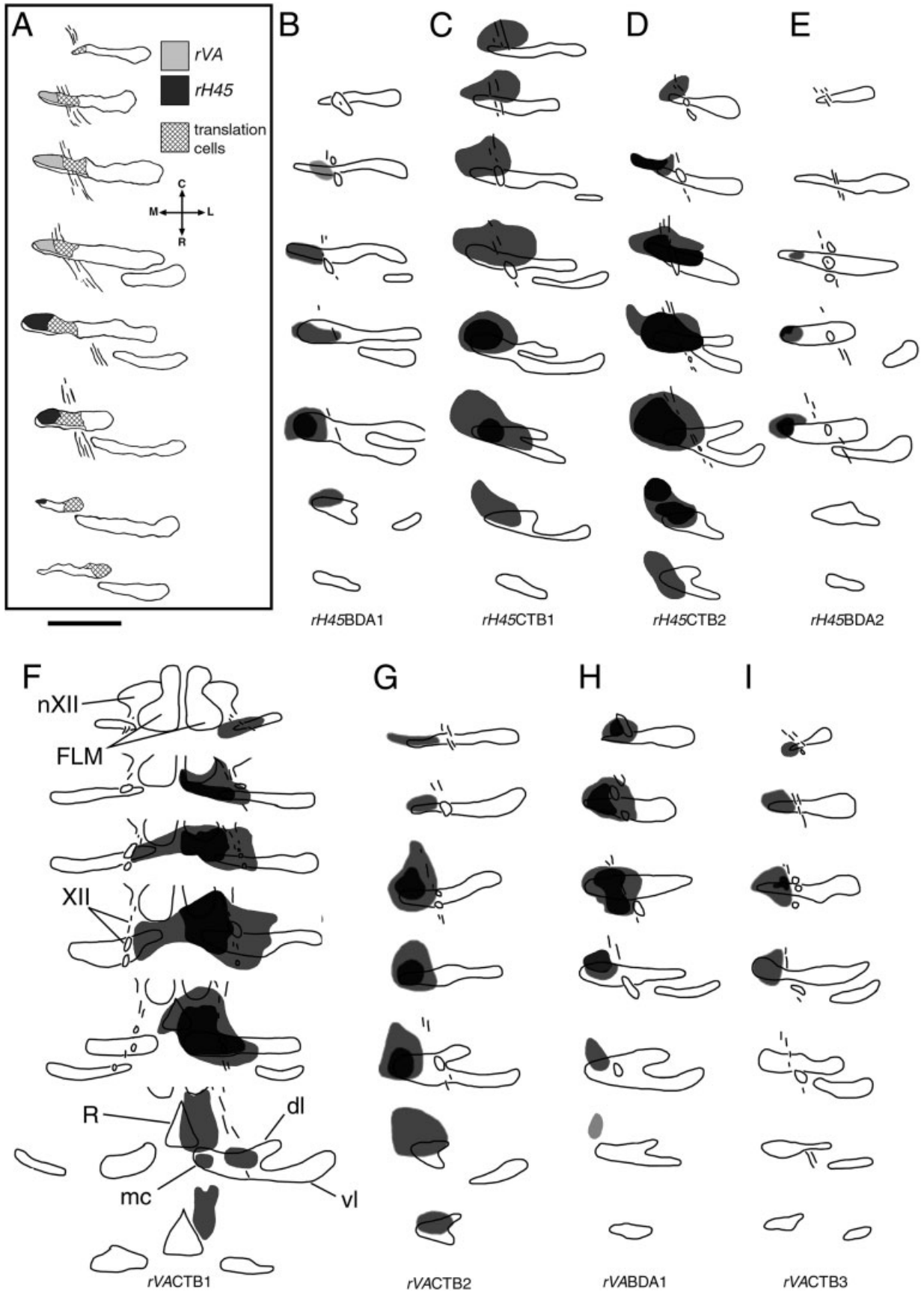


Figure 5

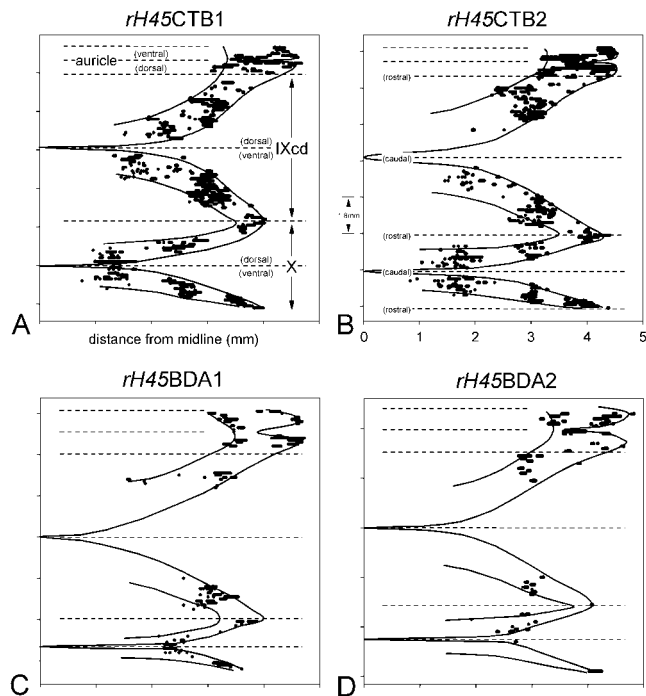


Fig. 6. Labeled climbing fibers (CFs) in the flocculus contralateral to the *rH45* injection sites. **A–D**: The location of anterogradely labeled CFs in the molecular layer are plotted for each *rH45* case. Both the distance from the midline and the rostrocaudal location are indicated. The radii of the Purkinje layers are indicated by the solid lines, and the dark dots show the location of labeled CFs.

### Case *rH45BDA2*

The injection site for this case is shown in Figure 5E. The injection site was very compact, centered in the medial margin of the *rH45* region and the spread was minimal. The location of anterogradely labeled CFs are plotted in Figure 6D. Little labeling was observed in folium X. In

Fig. 5. Injection sites at rotation-sensitive neurons in the medial column of the inferior olive (mcIO). **A**: The functional topography of neurons sensitive to translational and rotational optic flow in the mcIO from previous neuroanatomic and electrophysiological studies (Lau et al., 1998; Wylie et al., 1999; Crowder et al., 2000; Winship and Wylie, 2001). The mcIO is that part of the IO medial to the fibers of the twelfth cranial nerve (XII). The rostral and caudal areas of the medial part of the mcIO, contain *rH45* and *rVA* neurons, which are shown by the dark gray and light gray shading, respectively (Wylie et al., 1999; Winship and Wylie, 2001). The regions of the mcIO lateral to the *rVA* and *rH45c* regions contain the neurons that are sensitive to translational optic flow (cross-hatching). The topographic organization of the mcIO illustrated in A was useful for predicting which regions of the mcIO were involved in the injection because of spread of the tracer outside the target area. Tracings (caudal to rostral, each section approximately 260  $\mu$ m apart) of the injection sites from all eight experiments are illustrated in **B–I**. The black shading indicates the centers of the injections, and the surrounding gray indicates the apparent spread. **B–E** illustrated injections at sites where *rH45* responses were recorded, whereas *rVA* responses were recorded at the injection sites illustrated in **F–I**. C, R, M, and L = caudal, rostral, medial, and lateral, respectively. XII, twelfth cranial nerve. For other abbreviations, see list. Scale bar = 500  $\mu$ m in A (applies to A–I).

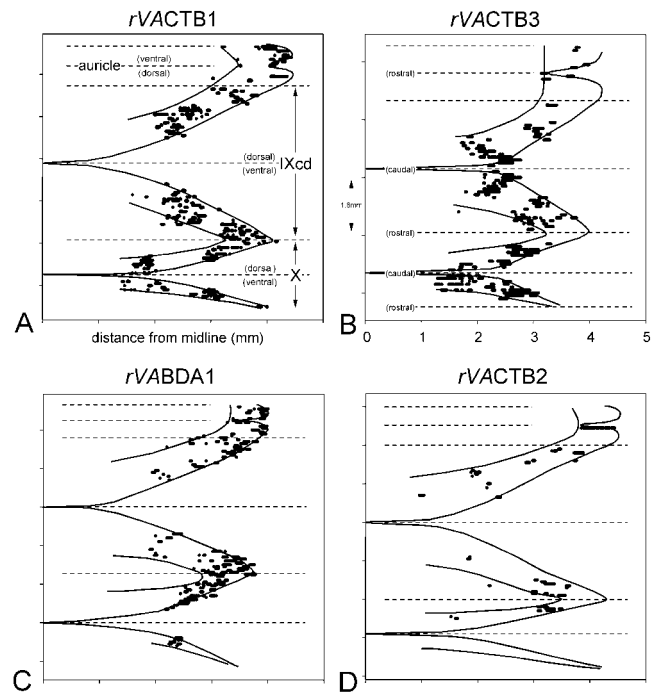


Fig. 7. Labeled climbing fibers (CFs) in the flocculus contralateral to the *rVA* injection sites. See caption to Figure 6 for details.

ventral X, there was only one section that contained anterogradely labeled CFs. These were located at the lateral extreme and are consistent with the lateral zone labeling from the other 3-*rH45* cases. In dorsal X, there was a group of CFs centered approximately 2.75 mm from the midline, corresponding to the medial zone labeling from the other three cases. Two zones were found in folium IXcd: a rostralateral zone occupying the auricle, and a second mediocaudal zone centered approximately 3.1 mm from the midline. For this case, no CF labeling was found in other folia.

### Summary of *rH45* injections

In Figure 4A, the four *rH45* cases are collapsed. Because of the variability in the size of the across birds, especially with respect to folium X, the rostrocaudal and mediolateral dimensions were first normalized. The width of folium X was normalized to 80% of the lateral edge of the auricle. The medial zones from the CTB cases, which we proposed are due to spread of the injections to the translation regions, have been omitted. Two clear zones in the flocculus emerge: one at rostralateral extent of folia IXcd and X and extending through the auricle, and a second caudomedial zone. The sparse labeling medially in folium IXcd is from the two CTB cases and could be due to spread of the injections beyond the *rH45* region, caudally into the *rVA* region.

### Case *rVACTB1*

This injection site, shown in Figure 5F was very large and heavy, with tracer spread extending to the contralateral (left) mcIO. The injection site was centered on the medial margin of the *rVA* region in the right mcIO, but

spread rostrally to include much of the *rH45* area, and laterally, incorporating the translation areas and parts of the dorsal lamella. On the left side of the cerebellum, heavy anterogradely labeling was seen throughout the flocculus, ventral uvula and nodulus, and the C and E zones of folia II-IXab. Fainter labeling was observed in the A zone across folia VIII and IXab. Because of the abundance of CF labeling and that the injection site included both the *rVA* and *rH45* regions of the right IO, the CF labeling on the left side of the cerebellum was not considered.

In the left mcIO, the spread of the injection appeared to be confined to the *rVA* region. CF labeling on the right side of the cerebellum was confined to the flocculus and is plotted in Figure 7A. In folium X, two zones were observed: a caudomedial zone and rostralateral zone centered 1.8 and 3.1 mm from the midline, respectively. Note that the rostralateral margin was basically devoid of labeled CFs. There were also two large zones in folium IXcd: a caudomedial group was centered 2.3 mm from the midline and a rostralateral group that was more prominent in ventral IXcd. There was some labeling in the auricle, but it was sparse, particularly in dorsal IXcd.

### Case *rVACTB2*

The injection in case *rVACTB2*, shown in Figure 5G, was centered on the mediorostral margin of the *rVA* region of the mcIO. Tracer spread rostrally into the *rH45* region and may have encroached laterally on the translation regions. The locations of anterogradely labeled CFs in the vestibulocerebellum are plotted in Figure 7D. Despite a significant injection and apparent spread, a poverty of labeling was observed in the flocculus relative to other CTB injections. In folium X, only one large group of labeled fibers, centered 3.3 mm from the midline and a second small group of fibers near the translation/rotation border (1.6 mm from the midline) were observed. Two groups of fibers were observed in folium IXcd; one zone caudomedial to the auricle and centered 3.3 mm from the midline, and a second sparse zone found mediocaudally near the translation/rotation border, 2.0 mm from the midline. Labeled CFs were also observed in a single section in the dorsal auricle.

Elsewhere in the cerebellum, labeled CF terminals were seen laterally in folia IXab and VIII (zone E). Faintly labeled CFs were also seen in the C and E zones of folium VII.

### Case *rVACTB3*

The injection in case *rVACTB3*, shown in Figure 5I, was centered on the *rVA* region of the mcIO, with little spread into adjacent regions but possibly encroaching the medial margins of the translation region. Anterogradely labeled CFs in the vestibulocerebellum are plotted in Figure 7B. Folium X was quite small in this animal, but two zones are apparent: a mediocaudal zone and a rostralateral zone, centered 1.8 mm and 3.1 mm from the midline, respectively. Two bands of fibers are observed folium IXcd; one rostralateral zone centered 3.1 mm from the midline, and a second mediocaudal zone centered 2.3 mm from the midline.

Labeled CFs were also found 0.15–0.4 mm from the midline in the nodulus and ventral uvula, consistent with spread of the injection from the caudal regions of the translation region of mcIO (Crowder et al., 2000), but

these fibers were not plotted in Figure 7B. Some labeled CFs were also seen in zone E of folia VIII and IXab, and a few faintly labeled CFs were seen in the C zone of these folia.

### Case *rVABDA1*

This injection site, illustrated in Figure 5H, was centered on the *rVA* region, with spread encroaching rostrally on the *rH45* region and laterally on the translation regions. Anterogradely labeled CFs in the flocculus are plotted in Figure 7C. In folium X, a single band of CFs was observed. This band was more diffuse in dorsal X. There is a suggestion of two bands in folium IXcd: a rostralateral zone, which spills into the auricle, and a smaller second zone medial and caudal to this zone centered 2.2 mm from the midline. There is a clear space between the two zones. CF labeling outside the flocculus was not observed.

### Summary of *rVA* injections

In Figure 4B, the five *rVA* cases are normalized and collapsed. In folium X, two zones emerge: a rostralateral zone and a caudomedial zone. The data for folium IXcd are not as clear, but there is a suggestion of caudomedial and rostralateral zones.

In Figure 4C, the data from the *rH45* cases (i.e., Fig. 4A) is superimposed on top of the data from the *rVA* cases (i.e., Fig. 4B). *rH45* and *rVA* data are represented by light gray and black circles, respectively. The two *rH45* zones are interdigitated with two *rVA* zones. This finding is most convincing for folium X, where there is little overlap of the zones but also apparent in folium IXcd. Starting medio-caudally and moving rostralaterally, an *rVA* zone is followed by an *rH45* zone, a second *rVA* zone, and an *rH45* zone, which occupies the auricle.

## DISCUSSION

In the present study, anterograde tracers were iontophoretically injected into physiologically identified rotation-sensitive optic flow regions in the mcIO in pigeons. The locations of anterogradely labeled CFs were then measured to determine the zonal organization of rotation-sensitive Purkinje cells in the flocculus. A clear zonal organization spanning both folium IXcd and X was revealed, consisting of two *rVA* zones interdigitated with two *rH45* zones. The zonal organization is idealized in Figure 8. In this figure, the *rVA* and *rH45* zones were superimposed on a representative set of tracings through the cerebellum. Borders between zones were delineated based on the normalized data presented in Figure 4. Dark gray and light gray shading are used to indicate the approximate position of *rVA* and *rH45* zones, respectively. This summary is cleaner than the actual data presented in Figures 4, 6, and 7. However, we did have to contend with spread outside of the target areas (see Fig. 5) and a high degree of variability in the size and shape of folia IXcd and X between birds (see Figs. 6, 7).

Electrophysiological studies provide some support for this zonal organization. In the companion paper (Wylie et al., 2003), small deposits of anterograde tracers were made at locations where *rVA* and *rH45* CSA was recorded. The locations of the injections were then plotted on the summary shown in Figure 8. Although this was a small data set, there was 100% concordance: *rVA* CSA was recorded in the *rVA* zones, and *rH45* CSA was recorded in

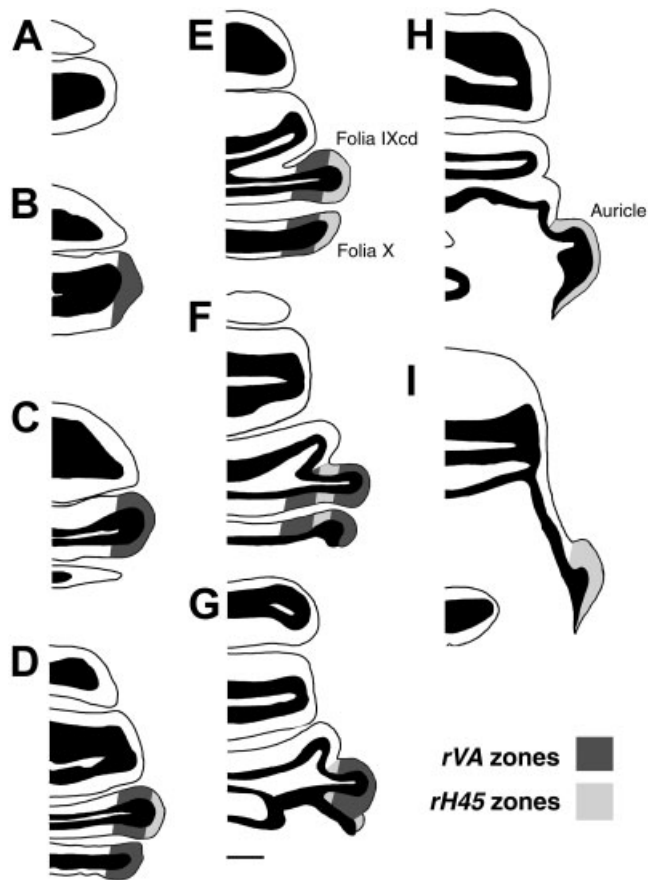


Fig. 8. Zonal organization of the pigeon flocculus. In this figure, optic flow zones were superimposed on a representative set of tracings through the vestibulocerebellum. A–I: Caudal to rostral, each approximately 440  $\mu\text{m}$  apart. Borders between zones were delineated based on the normalized data presented in Figure 4. Dark gray and light gray shading is used to indicate the approximate position of *rVA* and *rH45* zones, respectively. Scale bar = 1 mm in G (applies to A–G).

the *rH45* zones (see Fig. 4 of Wylie et al., 2003). There is also support from the electrophysiological study by Wylie et al. (1993). This study consisted of a much larger data set of CSA recordings in the vestibulocerebellum, although there were no recordings from the auricle (i.e., the rostromedial *rH45* zone). There are two apparent *rVA* zones: one just lateral to the CSA responsive to translational optic flow, and a second zone located more laterally. In between the two zones, *rH45* CSA was recorded, consistent with the caudomedial *rH45* zone revealed in the present study.

#### CTB and the potential problem of uptake by fibers of passage

Previous reports have shown that CTB can be taken up by fibers of passage (e.g., Chen and Aston-Jones, 1995), but we believe this does not pose a problem for the present study for several reasons. First, the fibers from the mcIO pass through the contralateral mcIO at the same rostrocaudal level. If fibers of passage took up the tracer, we would have seen CF terminals in the cerebellum ipsilateral to the injection site and retrogradely labeled cells in

the contralateral IO. A close examination of the sections revealed that there indeed were some retrogradely labeled cells scattered throughout the contralateral and ipsilateral IO. (Most were found at the same rostrocaudal level as the injection.) However, these cells were very lightly stained. Neurons in pretectum and nucleus of the basal optic root, which project to the mcIO (Wylie, 2001), were very darkly stained in the same brains. With regard to the presence of anterogradely labeled CFs ipsilateral to the injection site, we examined the route of the ipsilateral OCT in these sections. Although we saw numerous faintly labeled fibers in the brainstem, at the level of the dorsolateral vestibular nucleus, few fibers were labeled and they were extremely faint. Moreover, excluding case *rVACTB1* where the injection spread across the midline, no CF terminals were observed in the molecular layers ipsilateral to the injection site. Second, for the present study, the labeling of fibers of passage only poses a problem if, for example, an injection in the *rVA* region in the caudal mcIO labeled fibers originating from cells in the *rH45* region in the rostral mcIO. However, we found that the fibers from the injection crossed the midline directly, rather than traveling rostral or caudally before crossing the midline (see Fig. 3B). Third, if uptake by fibers of passage had been a problem, we would not have seen the complimentary pattern of labeling that we saw from the *rVA* and *rH45c* injections. The data in this regard were quite clear-cut, particularly for folium X (Fig. 4). Surely the data would have been noisier if uptake by fibers of passage posed a significant problem. Indeed, we believe that the minimal overlap we did see was due from spread of the injection site beyond the intended target area. Finally, the results from the BDA experiments are in concordance with the CTB experiments. The BDA injections were quite localized and uptake by fibers of passage did not seem to pose much of a problem. Although a few (< a dozen in each case) retrogradely labeled cells were seen in the mcIO contralateral to the injection site, no fibers were seen in the ipsilateral OCT and no CF terminals were seen ipsilateral cerebellar cortex. Moreover, contralateral to the injection site, only a single CF terminal was found outside the flocculus in the three BDA cases. In summary, a close examination of our tissue strongly suggests that uptake by fibers did not pose a significant problem.

#### Comparison with the zonal organization of the mammalian flocculus

Tan et al. (1995) used anterograde transport from the IO to identify the organization of CF inputs from the IO to flocculus in rabbits. They showed that CF inputs from the rostral dc and vlo, which contain *rH45* neurons (Leonard et al., 1988) terminated in two parasagittal zones (FZ<sub>I</sub> and FZ<sub>III</sub>), whereas inputs from the caudal dc, which contains *rVA* neurons (Leonard et al., 1988), terminated in two parasagittal zones (FZ<sub>II</sub> and FZ<sub>IV</sub>). Acetylcholinesterase histochemistry showed that olivocerebellar fibers innervating floccular zones FZ<sub>I</sub> and FZ<sub>III</sub> or FZ<sub>II</sub> and FZ<sub>IV</sub> traversed the white matter compartments FC<sub>I</sub> and FC<sub>III</sub> or FC<sub>II</sub> and FC<sub>IV</sub>, respectively, before terminating in the molecular layer. CSA in the rabbit flocculus in response to optokinetic stimulation also supports this organization: *rVA* CSA is found in zones FZ<sub>II</sub> and FZ<sub>IV</sub>, whereas *rH45* CSA is found in zones FZ<sub>I</sub> and FZ<sub>III</sub> (Kusunoki et al., 1990; De Zeeuw et al., 1994).

The zonal organization of the flocculus in cats and rats closely resembles that of rabbits. The rat flocculus can be divided into four parasagittal strips: two zones receiving CF input from the caudal dc interdigitated with one zone receiving CF input strictly from the vlc and another zone receiving a projection from the rostral dc and vlc (Ruigrok et al., 1992). In cats, Gerrits and Voogd (1982) distinguished six floccular climbing fiber zones (F1-F6) and a seventh zone, F7, in the medial extension. Zones F1 and F4 of the cat are identical to FZ<sub>II</sub> and FZ<sub>IV</sub> in the rabbit (Tan et al., 1995; Voogd et al., 1996). FZ<sub>I</sub> and FZ<sub>III</sub> of the rabbit flocculus are subdivided further in the cat. FZ<sub>I</sub> consists of zones F5 + 6 + 7 in the cat (found medially), and zone FZ<sub>III</sub> is divided into subzones F2 + 3 (found laterally). F1 and F4 receive CF input from the caudal dc, zones F3 and F6 from the rostral dc, and zones F2 and F5 are innervated by the vlc.

Data on the zonal organization of the primate flocculus is less conclusive than that of the cat, rat, rabbit, and pigeon. Acetylcholinesterase histochemistry in the macaque cerebellum has revealed white matter compartments in the flocculus and paraflocculus (Hess and Voogd, 1986; Voogd et al., 1987a,b). Three compartments restricted to the flocculus and ventral paraflocculus appear to correspond zones FC<sub>I-III</sub> of the rabbit (Voogd et al., 1987a,b). Olivocerebellar fibers in the middle compartment of the flocculus and the ventral paraflocculus have been identified by using injections of tritiated leucine in the caudal dc of the macaque (Voogd et al., 1987a,b). However, an equivalent to FZ<sub>IV</sub> of the rabbit flocculus has not been identified in primates.

In the present study, we show that the zonal organization in the flocculus of the pigeons is quite similar to that in mammalian species, particularly rabbits, and this pattern of interdigitation of *rVA* and *rH45* zones seems highly conserved. Although the order of the zones presented here in pigeons appears to be reversed in transverse sections or reconstructions of the flocculus of rabbits (insofar as the most medial section appears to be an *rH45* region in rabbits and *rVA* in pigeons), this reversal in fact represents the differing topology of the avian and mammalian flocculus. In mammals, the area of the vestibulocerebellum (VbC) containing the flocculus, termed the terminal hook, is folded back upon itself (Bolk, 1906, cited in Glickstein and Voogd, 1995; Voogd and Glickstein, 1998; Nieuwenhuys et al., 1998). As a result, the order of zones viewed in transverse sections becomes reversed compared with the pigeon, where such a topologic transformation does not occur.

There are some differences with respect to the olivocerebellar input to the flocculus. In rabbits some of the CFs innervating the flocculus send collaterals to the ventral uvula and nodulus (Takeda and Maekawa, 1989a,b). Consistent with this, CSA in the ventral uvula and nodulus of rabbits responds to rotational optic flow. There are two *rVA* zones on either side of an *rH45* zone (Kusonoki et al., 1990; Wylie et al., 1995). In pigeons, it has been shown that the CSA in the ventral uvula and nodulus responds best to patterns of translational optic flow (Wylie et al., 1993, 1998; Wylie and Frost, 1993, 1999a) and the olivary input to the translation zones is from cells that reside lateral to the floccular projecting cells in the mcIO (Lau et al., 1998; Wylie et al., 1999; Crowder et al., 2000). We have suggested previously that the translation zones in the pigeon vestibulocerebellum are analogous to the most me-

dial zone in the rabbit ventral uvula and nodulus (Lau et al., 1998; Crowder et al., 2000). Purkinje cells in this zone receive climbing fiber input from the beta subnucleus of the IO and are responsive to head tilt originating in the otolith organs (Shojaku et al., 1991; Barmack and Shojaku, 1992, 1995). What this zone has in common with the translation zones in the pigeon VbC is that both would be active during self-translation. In the companion paper (Wylie et al., 2003), we show that there are differences between rabbits and pigeons with respect to the output of floccular Purkinje cells in the *rVA* and *rH45* zones.

## LITERATURE CITED

- Arends JJA, Voogd J. 1989. Topographic aspects of the olivocerebellar system in the pigeon. *Exp Brain Res Suppl* 17:52-57.
- Arends JJA, Zeigler HP. 1991. Organization of the cerebellum in the pigeon (*Columba livia*): I. Corticonuclear and corticovestibular connections. *J Comp Neurol* 306:221-244.
- Barmack NH, Shojaku H. 1992. Representation of a postural coordinate system in the nodulus of the rabbit cerebellum by vestibular climbing fiber signals. In: Shimazu H, Shimoda Y, editors. *Vestibular control of eye, head and body movements*. Basel: Japan Scientific Societies Press. p 331-338.
- Barmack NH, Shojaku H. 1995. Vestibular and visual climbing fiber signals evoked in the uvula-nodulus of the rabbit cerebellum by natural stimulation. *J Neurophysiol* 74:2573-2589.
- Chen S, Aston-Jones G. 1995. Evidence that cholera toxin B subunit (CTB) can be avidly taken up and transported by fibers of passage. *Brain Res* 674:107-111.
- Crowder NA, Winship IR, Wylie DRW. 2000. Topographic organization of inferior olive cells projecting to translational zones in the vestibulocerebellum of pigeons. *J Comp Neurol* 419:87-95.
- De Zeeuw CI, Wylie DR, DiGiorgi PL, Simpson JI. 1994. Projections of individual Purkinje cells of physiologically identified zones in the flocculus to the vestibular and cerebellar nuclei in the rabbit. *J Comp Neurol* 349:428-447.
- Ezure K, Graf W. 1984. A quantitative analysis of the spatial organization of the vestibulo-ocular reflexes in lateral and frontal-eyed animals. I. Orientation of semicircular canals and extraocular muscles. *Neuroscience* 12:85-93.
- Freedman SL, Voogd J, Vielvoye GJ. 1977. Experimental evidence for climbing fibers in the avian cerebellum. *J Comp Neurol* 175:243-252.
- Gerrits NM, Voogd J. 1982. The climbing fiber projection to the flocculus and adjacent paraflocculus in the cat. *Neuroscience* 7:2971-2991.
- Glickstein M, Voogd J. 1995. Lodewijk Bolk and the comparative anatomy of the cerebellum. *Trends Neurosci* 18:206-210.
- Graf W, Simpson JI, Leonard CS. 1988. Spatial organization of visual messages of the rabbit's cerebellar flocculus. II. Complex and simple spike responses of Purkinje cells. *J Neurophysiol* 60:2091-2121.
- Hess DT, Voogd J. 1986. Chemoarchitectonic zonation of the monkey cerebellum. *Brain Res* 369:383-387.
- Karten HJ, Hodos W. 1967. A stereotaxic atlas of the brain of the pigeon (*Columba livia*). Baltimore: Johns Hopkins Press.
- Kusonoki M, Kano M, Kano M-S, Maekawa K. 1990. Nature of optokinetic response and zonal organization of climbing fiber afferents in the vestibulocerebellum of the pigmented rabbit. I. The flocculus. *Exp Brain Res* 80:225-237.
- Larsell O. 1948. The development and subdivisions of the cerebellum of birds. *J Comp Neurol* 89:123-190.
- Larsell O, Whitlock DG. 1952. Further observations on the cerebellum of birds. *J Comp Neurol* 97:545-566.
- Lau KL, Glover RG, Linkenhoker B, Wylie DRW. 1998. Topographical organization of inferior olive cells projecting to translation and rotation zones in the vestibulocerebellum of pigeons. *Neuroscience* 85:605-614.
- Leonard CS, Simpson JI, Graf W. 1988. Spatial organization of visual messages of the rabbit's cerebellar flocculus. I. Typology of inferior olive neurons of the dorsal cap of Kooy. *J Neurophysiol* 60:2073-2090.
- Nieuwenhuys R, Donkelaar HJ, Nicholson C. 1998. *The central nervous system of vertebrates*. Berlin: Springer-Verlag.
- Ruigrok TJH, Osse RJ, Voogd J. 1992. Organization of inferior olivary projections to the flocculus and ventral paraflocculus of the rat cerebellum. *J Comp Neurol* 316:129-150.

- Shojaku H, Barmack NH, Mizukoshi K. 1991. Influence of vestibular and visual climbing fiber signals on Purkinje cell discharge in the cerebellar nodulus of the rabbit. *Acta Otolaryngol Suppl* 481:242–246.
- Simpson JI, Graf W. 1981. Eye-muscle geometry and compensatory eye movements in lateral eyed and frontal-eyed animals. *Ann N Y Acad Sci* 374:20–30.
- Simpson JI, Graf W. 1985. The selection of reference frames by nature and its investigators. In: Berthoz A, Melvill-Jones G, editors. *Adaptive mechanisms in gaze control: facts and theories*. Amsterdam: Elsevier. p 3–16.
- Simpson JI, Graf W, Leonard CS. 1981. The coordinate system of visual climbing fibers to the flocculus. In: Fuchs AF, Becker W, editors. *Progress in oculomotor research*. Amsterdam: Elsevier. p 475–484.
- Simpson JI, Leonard CS, Soodak RE. 1988a. The accessory optic system: analyzer of self-motion. *Ann N Y Acad Sci* 545:170–179.
- Simpson JI, Leonard CS, Soodak RE. 1988b. The accessory optic system: II. Spatial organization of direction selectivity. *J Neurophysiol* 60:2055–2072.
- Simpson JI, Graf W, Leonard CS. 1989a. Three-dimensional representation of retinal image movement by climbing fiber activity. In: Strata P, editor. *The olivocerebellar system in motor control: experimental brain research supplement*. Vol. 17. Heidelberg: Springer-Verlag. p 323–327.
- Simpson JI, Van der Steen J, Tan J, Graf W, Leonard CS. 1989b. Representations of ocular rotations in the cerebellar flocculus of the rabbit. *Prog Brain Res* 80:213–223.
- Takeda T, Maekawa K. 1989b. Olivary branching to the flocculus, nodulus and ventral uvula in the rabbit. I. An electrophysiological study. *Exp Brain Res* 74:47–62.
- Takeda T, Maekawa K. 1989a. Olivary branching to the flocculus, nodulus and ventral uvula in the rabbit. II. Retrograde double labeling study with fluorescent dyes. *Exp Brain Res* 76:323–332.
- Tan J, Gerrits NM, Nanhoe RS, Simpson JI, Voogd J. 1995. Zonal organization of the climbing fiber projection to the flocculus and nodulus of the rabbit. A combined axonal tracing and acetylcholinesterase histochemical study. *J Comp Neurol* 356:23–50.
- van der Steen J, Simpson JI, Tan J. 1994. Functional and anatomic organization of three-dimensional eye movements in rabbit cerebellar flocculus. *J Neurophysiol* 72:31–46.
- Veenman CL, Reiner A, Honig MG. 1992. Biotinylated dextran amine as an anterograde tracer for single- and double-labeling studies. *J Neurosci Methods* 41:239–254.
- Voogd J, Glickstein M. 1998. The anatomy of the cerebellum. *Trends Neurosci* 21:370–375.
- Voogd J, Gerrits NM, Ruigrok TJH. 1996. Organization of the vestibulocerebellum. *Ann N Y Acad Sci* 781:553–579.
- Voogd J, Gerrits NM, Hess DT. 1987a. Parasagittal zonation of the cerebellum in Macaques: an analysis based on acetylcholinesterase histochemistry. In: Glickstein M, Yeo Ch, Stein J, editors. *Cerebellum and neuronal plasticity*. New York: Plenum. p 15–39.
- Voogd J, Hess DT, Marani E. 1987b. The parasagittal zonation of the cerebellar cortex in cat and monkey. Topography, distribution of acetylcholinesterase and development. In: King JS, editor. *New concepts in cerebellar neurobiology*. New York: Liss. p 15.
- Whitlock DG. 1952. A neurohistological and neurophysiological study of afferent fiber tracts and receptive areas of the avian cerebellum. *J Comp Neurol* 97:567–635.
- Wild JM. 1993. Descending projections of the songbird nucleus robustus archistrialis. *J Comp Neurol* 338:225–241.
- Winship IR, Wylie DRW. 2001. Responses of neurons in the medial column of the inferior olive in pigeons to translational and rotational optic flowfields. *Exp Brain Res* 141:63–78.
- Wylie DRW. 2001. Projections from the nucleus of the basal optic root and nucleus lentiformis mesencephali to the inferior olive in pigeons (*Columba livia*). *J Comp Neurol* 429:502–513.
- Wylie DR, Frost BJ. 1993. Responses of pigeon vestibulocerebellar neurons to optokinetic stimulation: II. The 3-dimensional reference frame of rotation neurons in the flocculus. *J Neurophysiol* 70:2647–2659.
- Wylie DRW, Frost BJ. 1996. The pigeon optokinetic system: visual input in extraocular muscle coordinates. *Vis Neurosci* 13:945–953.
- Wylie DRW, Frost BJ. 1999a. Complex spike activity of Purkinje cells in the ventral uvula and nodulus of pigeons in response to translational optic flowfields. *J Neurophysiol* 81:256–266.
- Wylie DRW, Frost BJ. 1999b. Responses of neurons in the nucleus of the basal optic root to translational and rotational flowfields. *J Neurophysiol* 81:267–276.
- Wylie DR, Kripalani T-K, Frost BJ. 1993. Responses of pigeon vestibulocerebellar neurons to optokinetic stimulation: I. Functional organization of neurons discriminating between translational and rotational visual flow. *J Neurophysiol* 70:2632–2646.
- Wylie DR, De Zeeuw CI, Simpson JI. 1995. Temporal relations of the complex spike activity of Purkinje cell pairs in the vestibulocerebellum of rabbits. *J Neurosci* 15:2875–2887.
- Wylie DRW, Linkenhoker B, Lau KL. 1997. Projections of the nucleus of the basal optic root in pigeons (*Columba livia*) revealed with biotinylated dextran amine. *J Comp Neurol* 384:517–536.
- Wylie DRW, Bischof WF, Frost BJ. 1998. Common reference frame for neural coding of translational and rotational optic flow. *Nature* 392:278–282.
- Wylie DRW, Winship IR, Glover RG. 1999. Projections from the medial column of the inferior olive to different classes of rotation-sensitive Purkinje cells in the flocculus of pigeons. *Neurosci Lett* 268:97–100.
- Wylie DRW, Brown MR, Barkley RR, Winship IR, Todd KG. 2003. Zonal organization of the vestibulocerebellum in pigeons (*Columba livia*): II. Projections of the rotation zones of the flocculus. *J Comp Neurol* 456:140–153.